Analog experiments on magma-filled cracks: Competition between external stresses and internal pressure

Tohru Watanabe, Takayuki Masuyama, Kazuhiro Nagaoka, and Tsuyoshi Tahara

Department of Earth Sciences, Toyama University, Gofuku 3190, Toyama 930-8555, Japan

We have performed two series of analog experiments using gelatin to study the propagation of liquid-filled cracks in stressed medium. The first series was designed to study the competition between the external stress and the liquid excess pressure in controlling the propagation direction. We systematically controlled the external stress and the liquid excess pressure by changing the surface load and the liquid volume. An ascending crack progressively deflected to be perpendicular to the maximum tensile direction of the external stress. The degree of deflection depends on the ratio of the shear stress on a crack plane to the average liquid excess pressure. More deflection was observed for a crack with a larger ratio. No significant deflection was observed for the ratio less than 0.2. The volcanic activity in a compressional stress field might be understood in the context of this competition. The first series also demonstrated the importance of the gradient of the crack normal stress as a driving force for propagation. The vertical gradient of the gravitational stress generated by a mountain load can control the emplacement depth of magmas, and it might lead to the evolution of eruption style during the lifetime of a volcano. The second series was designed to study the three-dimensional interaction of two parallel buoyancy-driven cracks. The deflection of the second crack takes place, when the ratio of the shear stress generated by the first one to the average excess pressure of the second crack is larger than 0.2. If the second crack reaches the first one, the interaction can lead to the coalescence of two cracks. It has directivity: the region of coalescence extends more in the direction perpendicular to the first crack than in the direction parallel to it. It reflects the stress field around the first crack. This directivity might cause a characteristic spatial variation of magma chemistry through magma mixing.

1. Introduction

Propagation of a magma-filled crack is the dominant mechanism of magma transport in the Earth's lithosphere. Widespread occurrence of dikes is evidence for their importance in volcanism (e.g., Pollard and Muller, 1976), and crack propagation can transport magma as rapidly (∼1 m/s) as estimated from xenoliths (e.g., Sparks *et al.*, 1977). Physics of crack propagation is thus essential for a good understanding of magma supply to volcanoes.

Earlier works were mainly concerned with an equilibrium shape of a stationary magma-filled crack and its stability (Weertman, 1971; Pollard and Muller, 1976; Pollard and Holtzhausen, 1979; Maaløe, 1987). Later, dynamic aspects of a magma-filled crack were studied by combining fluid mechanics of magma flow, elastic deformation of country rock and fracture at a crack tip (Spence and Turcotte, 1985; Emerman *et al.*, 1986; Spence *et al.*, 1987; Lister, 1990, 1991; Lister and Kerr, 1991, Nakashima, 1993). These studies have shown that the viscous resistance is more important than the fracture resistance at a crack tip once the crack length becomes sufficiently large to ascend. In a series of paper (Lister, 1990; Lister, 1991; Lister and Kerr, 1991), Lister studied the behavior of a magma-filled crack in a density-stratified medium, and showed that the direction of

crack propagation changes from vertical to horizontal around the level of neutral buoyancy (LNB). Although these studies of a magma-filled crack illustrate basic physical principles, they are rather too simple for representing natural systems. They assumed a constant flux from magma sources. Recently, Mériaux and Jaupart (1998) and Ida (1999) extended the dynamic theory to couple the propagation of a magma-filled crack and the discharge from a magma source.

Lithospheric stresses strongly affect the crack propagation in two ways. First, the stress field governs the orientation of a crack plane. A crack plane tends to become perpendicular to the maximum tensile stress (e.g., Cotterell and Rice, 1980). Secondly, the gradient of the crack normal stress can contribute to the driving force for propagation (e.g., Takada, 1989). Many investigations have been done on the influence of the external stress generated by tectonic forces (e.g., Nakamura, 1977), topography (e.g., McGuire and Pullen, 1989) and pre-existing magma bodies (e.g., Takada, 1994a).

Previous studies overlooked the role of magma excess pressure in controlling the propagation direction of a crack. The stress around a crack is composed of the stress generated by magma excess pressure and the external stress generated by tectonic forces, etc. The crack orientation should be determined by the competition between magma excess pressure and external stresses. Recently, Muller *et al.* (2001) studied this competition by crack experiments in gelatin. However, since they performed experiments for a fixed liquid pressure,

the role of liquid excess pressure was not clearly shown.

In order to study the competition between the external stress and the liquid excess pressure, we first performed experiments of crack propagation in gelatin with systematically changing the external stress and the liquid excess pressure (Experiment 1). A part of the experimental result has been already published (Watanabe *et al.*, 1999). In this paper, we will present a comprehensive data set and summarize it in terms of the ratio of the shear stress on a crack plane to the average excess pressure. Secondly, we performed experiments on the interaction of two parallel buoyancy-driven cracks with various configurations (Experiment 2). While previous studies (e.g., Takada, 1994a, b) on crack interaction were limited to in two-dimension, we observed behaviours of cracks in three-dimension. Since the numerical approach is still hard to perform in three-dimension, we interpreted observations based on two-dimensional analytical stress distributions. We will discuss implications for ascent and emplacement of magmas in the Earth's lithosphere.

2.   Working Materials

We employed gelatin and silicon oil as a host medium and a crack-filling liquid, respectively. Several experimental works have been done on fluid-filled cracks, using analog materials like gelatin (Fiske and Jackson, 1972; Maaløe, 1987; Takada, 1990, 1994a; Heimpel and Olson, 1994, Muller *et al.*, 2001) and agar (Lister and Kerr, 1991). They investigated the three-dimensional shape of a fluid-filled crack (Pollard and Jackson, 1973; Hyndmann and Alt, 1987; Maaløe, 1987; Takada, 1990), the propagation velocity (Takada, 1990; Heimpel and Olson, 1994), the influence of the external stress on the propagation direction (Fiske and Jackson, 1972; Takada, 1994a, b; Muller *et al.*, 2001), and the influence of the density structure on the propagation direction (Lister and Kerr, 1991).

Gelatin is a transparent, brittle, viscoelastic solid with a low rigidity and a Poisson's ratio of nearly 0.5 (Takada, 1990; Heimpel and Olson, 1994). Its low rigidity allows the gravity to be significant in laboratory-scale models (Richards and Mark, 1966). We can easily make a fluid-filled crack in gelatin, and observe its three-dimensional behavior. However, when we apply laboratory results to realistic situations, we have to carefully check their applicability.

The fracture resistance of a crack tip is relatively large in gelatin (Takada, 1990). It dominates the resistant force to crack propagation in laboratories. On the other hand, in realistic situations, once a magma-filled crack begins to extend, the fracture resistance plays no significant role in the resistant force. Instead, the viscous drag of magma dominates the resistant force. Thus, we must take into account the difference in force balance (Lister and Kerr, 1991).

Gelatin is an isotropic and homogeneous medium, while real rocks contain numerous cracks. We have to understand the influence of those preexisting cracks before applying experimental results to realistic situations. Delaney *et al.* (1986) showed that magma can invade into cracks of any orientation if the magma pressure exceeds the maximum compressive stress. However, a crack may not be able to follow such a fracture for long. The crack could hop out of the existing fracture and into a direction controlled by the ambient stress (Rubin, 1995). Thus, the crack propagation in stressed gelatin can be applied to that in the lithosphere.

We prepared gelatin by making 1.0 wt% aqueous solution of gelatin powder (E-290, Miyagi Chemical Industrial Co. Ltd., Japan) and solidifying it in an acrylic container at 5°C for 2 days. All the experiments were performed at the room temperature. After an experiment of a couple of hours, the temperature of gelatin was still 6 ± 1°C in the middle. We thus think that the temporal change in material properties of gelatin was negligible during our experiments.

Gelatin adheres to the container wall. Thus, without any disturbance (e.g., surface load), the horizontal strains are nil in the gravitational stress. The horizontal (σ_x, σ_y) and vertical (σ_z) stresses are thus related as

$$\sigma_x = \sigma_y = \frac{\nu}{1 - \nu}\sigma_z \tag{1}$$

where ν is Poisson's ratio. Because Poisson's ratio is nearly 0.5, the stress condition in gelatin is nearly hydrostatic before disturbance.

The density of gelatin is 1008 ± 3 kg/m^3. Assuming that Poisson's ratio is 0.5, we estimated the rigidity to be about 270 Pa by comparing the theoretical (e.g., Lister and Kerr, 1991) and experimental shapes of fluid-filled cracks. Young's modulus is expected to be about 800 Pa, which is similar to the values obtained by Takada (1990). The silicon oil (KF-96L, Shin-Etsu Chemical Co. Ltd., Japan) has a density of 810 kg/m^3 and a viscosity of 1.2×10^{-3} Pa·s. In order to see the shape of a fluid-filled crack clearly, the silicon oil was dyed red.

3.   Experiment 1: Competition between External Stress and Liquid Excess Pressure

3.1   Method

Gelatin was prepared in a rectangular container (585 mm in width, 260 mm in depth and 350 mm in height), and a vertical liquid-filled crack was formed by injection of silicon oil from the bottom. The external stress was generated by a load (wood block: 90 mm in width and 200 mm in depth, various height) on the gelatin surface. The liquid excess pressure was controlled by changing the liquid volume in a crack. Changing the load and the liquid volume, we systematically studied the competition between the external stress and the liquid excess pressure in governing the propagation direction of a crack.

The stress in gelatin is two-dimensional and approximated to be that in a semi-infinite medium with a surface load except for the vicinity of container walls. The stress in a semi-infinite medium can be analytically evaluated (Appendix A). The direction of the maximum compressive stress and its contour is shown in Fig. 1. The hydrostatic stress component is omitted. The magnitude of the stress is normalized by the load per unit area, and the length by the half width of the load (45 mm). In our experiments, the load per unit area was of the order of 100 Pa. The direction of maximum compressive stress diverges radially from just below the center of the load. Photoelastic technique showed that the stress within gelatin is reasonably approximated by the analytic solution (Fig. 2).
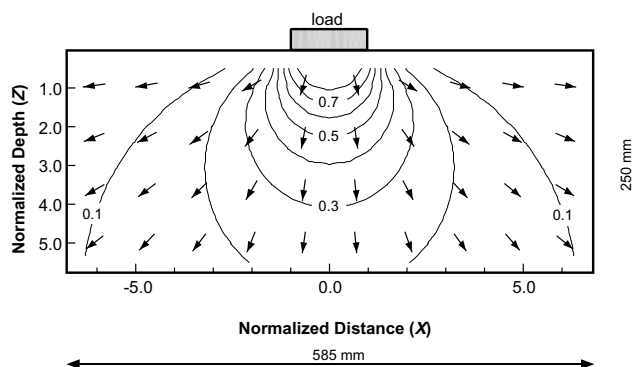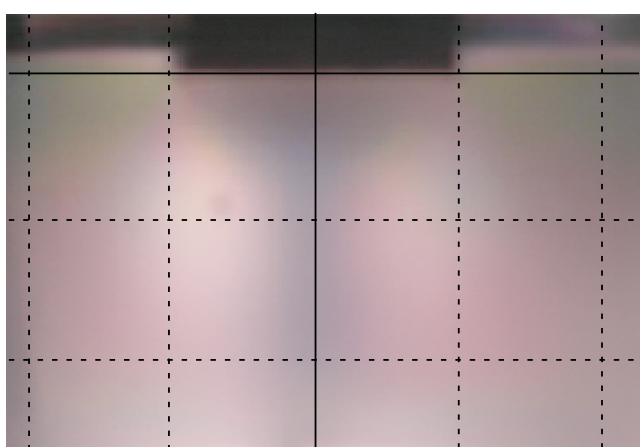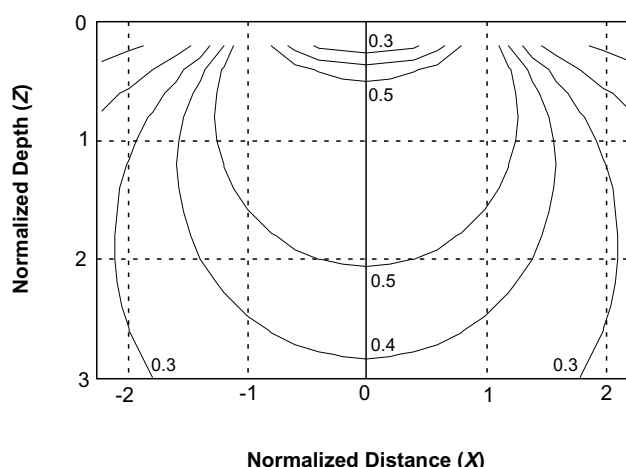
Fig. 1. The direction and contour of the maximum compressive stress generated by a surface load. The analytical solution to make this diagram is shown in Appendix A. The hydrostatic component of stresses is omitted. The magnitude of the stress is normalized by the load per unit area and the length by the half width of the load (45 mm).

(a)

(b)

Fig. 2. (a) Photoelastic stress field generated by a surface load (140 Pa per unit area). Colors reflect the magnitude of the differential stress within gelatin. The dark region separating the two bright lobes is an isogyre. It shows where light fails to penetrate the system since the directions of principal stresses coincide with the orientations of the crossed polarized sheets. (b) The contour of the differential stress (σ_1-σ_2) generated by a surface load. Stresses are calculated by using an analytical solution (Appendix A). The stress magnitude is normalized by the load per unit area and the length by the half width of the load.

The liquid excess pressure at the depth z is defined as

$$p_{ex}(z) = p_l(z) - \sigma(z) \qquad (2)$$

where p_l and σ are the liquid pressure and the normal stress to the crack, respectively. When the vertical gradient of the deviatoric stress is negligible, the average excess pressure in a vertical crack is approximated to be $\Delta\rho g L/4$ (Appendix B), where $\Delta\rho$, g and L are the density difference between the liquid and gelatin, the gravitational acceleration and the crack height. Dimensions of a crack are defined in Fig. 3. When the height L is 100 mm, the average excess pressure is around 50 Pa. We can control the average excess pressure by changing the liquid volume, since the height increases with the liquid volume. The approximation is valid when

$$\left| \frac{d\sigma'_{xx}}{dz} \right| \ll \rho_g g \qquad (3)$$

where σ'_{xx} and ρ_g are the deviatoric component of the crack normal stress and the density of gelatin. This condition is satisfied if the normalized depth of the crack upper tip is larger than 1 (Appendix B).

In each experiment, we first formed a vertical crack in gelatin before putting a surface load. The initial orientation of a crack was controlled by the needle of a syringe. We checked each time that a crack ascended vertically without a surface load. When the upper tip of the crack reached the depth of 120 mm ($Z = 2.7$ in Fig. 1), we put a surface load and then observed a crack path.

The load per unit area was varied as 70, 140 and 210 Pa. The liquid volume was varied as 15, 20 and 25 ml. The measured height of the crack was 75, 85 and 95 mm, respectively. The average liquid excess pressure is thus calculated to be 38, 43 and 48 Pa. We also changed the horizontal distance between the initial crack and the load. The horizontal distance from the center of a load was varied as 85, 125, 165 mm.

3.2 Results and discussion

3.2.1 Directional change After applying the external stress, a liquid-filled crack ascended with progressively de-
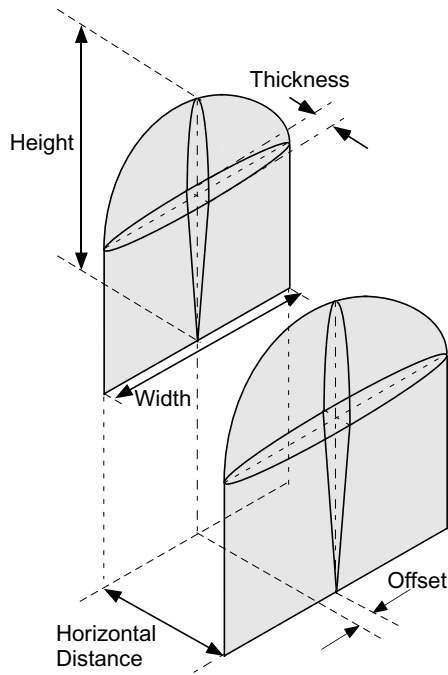
Fig. 3. A schematic drawing of two parallel and offset liquid-filled cracks. The height, width, thickness, horizontal distance and offset are measured as shown.

flecting from the vertical direction (Fig. 4). The observed paths of a crack upper tip are summarized in Fig. 5, where the depth and the distance are normalized by the half width of the load (45 mm). The contour of the shear stress σ_{zx} is also shown, which is normalized by the load per unit area. The ratio of the average excess pressure to the load per unit area was varied from 0.18 to 0.68.

A crack tends to be more deflected for smaller ratio of the average excess pressure to the load per unit area. Some exceptions ($\bar{p}_{ex}/p_{load} = 0.53$ in (a) and (b)) may be due to poor control in the initial direction by the needle. For the normalized initial distance of 1.9 (Fig. 5(a)), where the shear stress is relatively high, all cracks were deflected. The degree of deflection increases with decreasing ratio of the average excess pressure to the load per unit area. For the normalized initial distance of 3.7 (Fig. 5(c)), cracks with larger ratios (>0.35) of the average excess pressure to the surface load per unit area showed little deflection. Cracks with smaller ratios are more deflected. For a ratio of 0.18, cracks almost follow trajectories of the most compressive stress generated by the surface load (Fig. 6).

We summarize the deflection of a crack in terms of the shear stress acting on a crack plane and the average liquid excess pressure. Under the hydrostatic condition, no shear stress acts on a vertical crack plane. The crack ascends vertically, generating a horizontal tensile stress at the upper tip by the liquid excess pressure. When the external stress is applied, the shear imposed on a crack plane deflects the crack away from plane geometry (Lawn, 1993). No significant deflection was observed when the ratio of the shear stress to the average liquid excess pressure was lower than 0.2 (Fig. 5). Though the vertical propagation was also unstable in these cases, the growth rate of instability must have been

quite low. If the host material is isotropic, the stress field around a propagating tip controls the propagation direction. The critical ratio of 0.2 can be used as a criterion for crack deflection. The degree of deflection must also increase with the ratio of the shear stress to the average excess pressure in the lithosphere. The implication to volcanisms will be discussed in the Subsection 5.1.

3.2.2 Velocity change A drop in the ascent velocity was observed near the surface load. When a crack upper tip is sufficiently far from the load (see Fig. 4(a) for example), the ascent velocity is around 10 mm/min. When its upper tip approaches the surface load (Fig. 4(b)), the velocity gradually decreases. In order to clarify the influence of a surface load on the ascent velocity, we performed additional experiments of vertical ascent with various loads. The center of a load was just above a crack to keep its vertical ascent. The liquid volume was 15 ml, and a load was placed when the crack upper tip reached the depth of 120 mm ($Z = 2.7$ in Fig. 1).

The ascent of a crack upper tip is summarized in Fig. 7. Without a surface load, a crack ascends at a constant rate (∼6 mm/min.) to the gelatin surface. After a surface load is placed, a crack slows down its ascent at shallow depths (<50 mm) and then stops. Below the depth of 50 mm ($Z = 1.1$ in Fig. 1), no significant difference in the ascent velocity is observed between with and without the surface load. The gelatin surface deformed downward by 3∼7 mm. The depth was measured from the bottom of the load. A crack ceases its ascent at a deeper depth for a larger load.

The surface load generates a vertical gradient of crack normal stress, which provides negative buoyancy to the crack-filling liquid. The total negative buoyancy exerted on a crack comes from the integration of the vertical stress gradient along the crack height. The depth profile of the crack normal stress and the total negative buoyancy can be analytically evaluated (Appendix A) and shown in Fig. 8. For simplicity, we assume that the width and the thickness of a crack are constant along its height. Namely, a crack is assumed to be in the shape of a rectangular plate. Both the crack normal stress and the total negative buoyancy rapidly decrease their magnitude with depth over the length scale of the half-width of a surface load (45 mm).

The balance between the driving force and the resistant force determines the ascent velocity. If we assume that the resistant force is proportional to the ascent velocity and that the proportionality coefficient c is independent of the buoyancy, we calculate the ascent velocity v as

$$v = (\text{driving force})/c = (\text{buoyancy} - \text{negative buoyancy})/c.$$

The coefficient c can be determined from the result without load. Integrating the velocity, we obtain the ascent of a crack for various loads (Fig. 8(c)). Our simple calculation reasonably reproduces general features of experimental results (Fig. 7). It overestimated the total negative buoyancy by assuming a simple geometry of a crack. This could explain more gradual deceleration in our experiments. The adhesion of gelatin to the load (wood blocks) reinforces the gelatin surface, which results in the termination beneath the load. We conclude that the vertical stress gradient generated by a surface load causes the observed velocity change. The
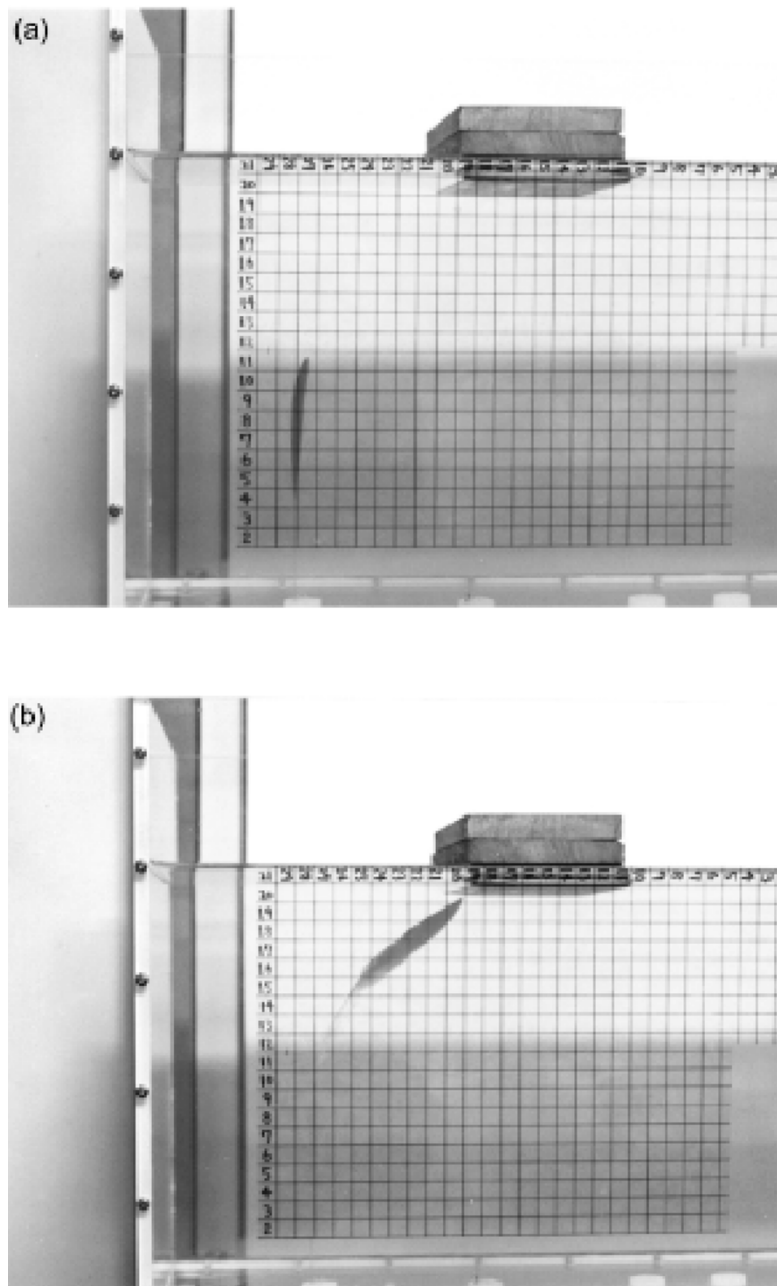
Fig. 4. Photographs showing the progressive deflection of crack orientation under the effect of a surface load. The surface load and the liquid volume were 210 Pa and 15 ml. The horizontal distance between the crack plane and the center of the load was initially 125 mm. (a) 10 minutes and (b) 90 minutes after putting the load. As approaching to the surface load, the ascent velocity decreases to zero. Little ascent was observed during the last 60 minutes.

calculation suggests that our assumption about the resistant force is not unreasonable.

Before closing this section, we discuss the property of resistant force in our experiments. Without a surface load, the driving force of crack-filling liquid is given by

$$f_b = \Delta \rho g V.$$

The density difference and the volume are 198 kg/m^3 and 1.5×10^{-5} m^3, respectively. The driving force is thus calculated to be 2.9×10^{-2} N. The resistant force is composed of viscous resistance and the fracture resistance. The magnitude of the viscous resistance is calculated to be 1.4×10^{-7} N, using

$$f_v = \eta \frac{v}{t} wh.$$

Therefore, the fracture resistance should be dominant in the resistant force, and be proportional to the velocity. Its proportionality coefficient seems to be insensitive to the driving force. We should stress that characteristics of resistant forces are specific to our experiments. The viscous resistance must dominate the resistant force in the lithosphere. However, the gradient of the crack normal stress can affect the ascent velocity also in realistic situations.

4. Experiment 2: Coalescence of Two Liquid-Filled Cracks

4.1 Interaction of two liquid-filled cracks

A liquid-filled crack itself becomes a source of non-hydrostatic stresses. It can affect the propagation of other
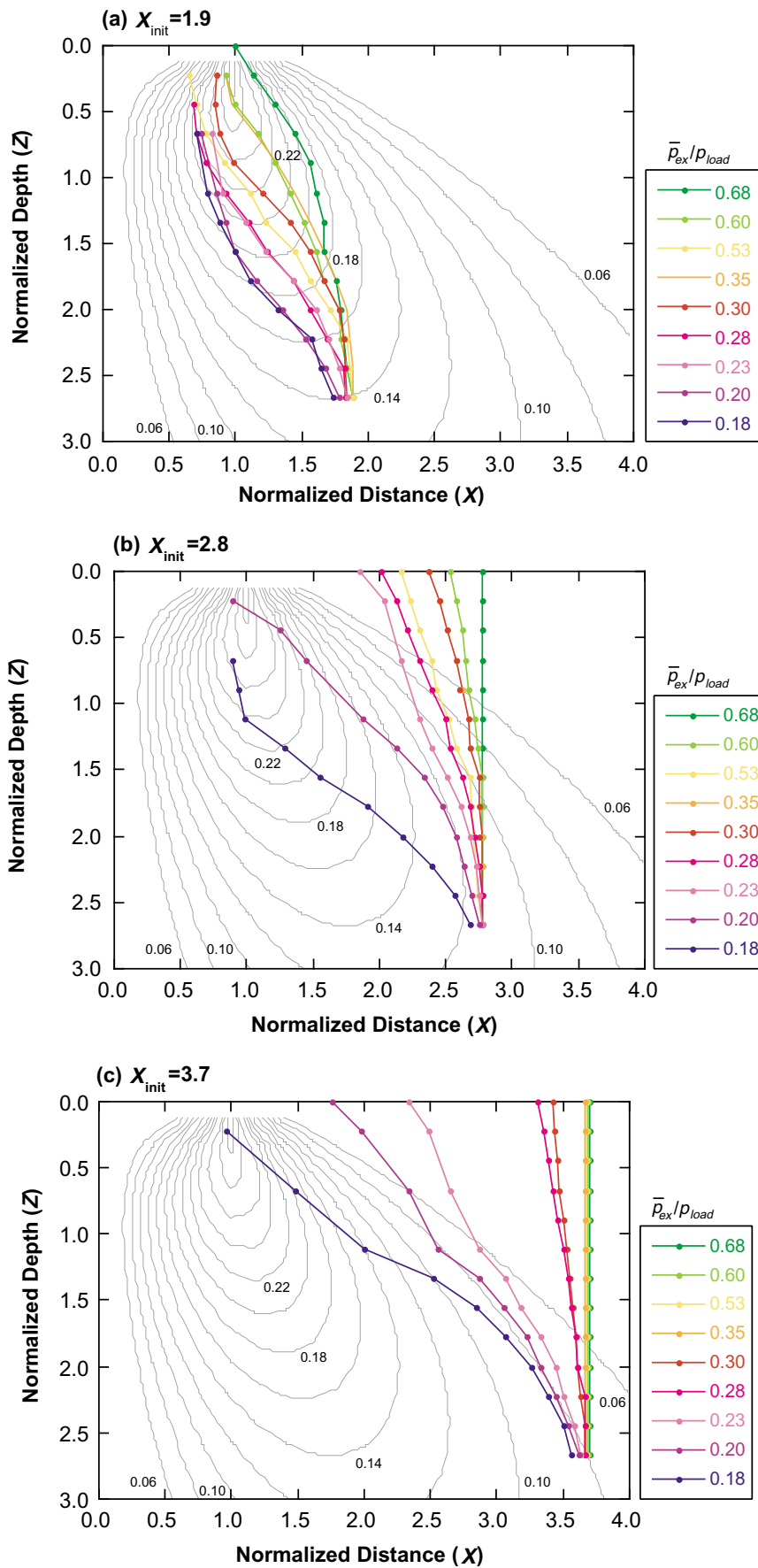
Fig. 5. The observed paths of a crack upper tip. The depth and the distance are normalized by the half width of the load (45 mm). The contour of the shear stress σ'_{zx}, which is calculated by using an analytical solution (Appendix A), is also shown. The shear stress is normalized by the surface load per unit area. The initial horizontal distance between the crack plane and the center of a load was varied as 85 mm (a), 125 mm (b), and 165 mm (c). The ratio of the average liquid excess pressure ($\bar{p}_{ex}$) to the surface load per unit area (p_{load}) was varied from 0.18 to 0.68.
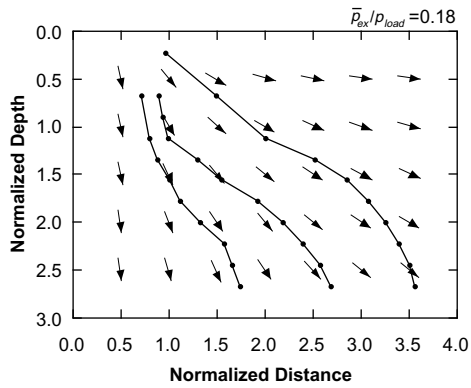
Fig. 6. The observed paths of a crack upper tip for the lowest average excess pressure ($\bar{p}_{ex}/p_{load} = 0.18$). The direction of the maximum compressive stress generated by the surface load is also shown.
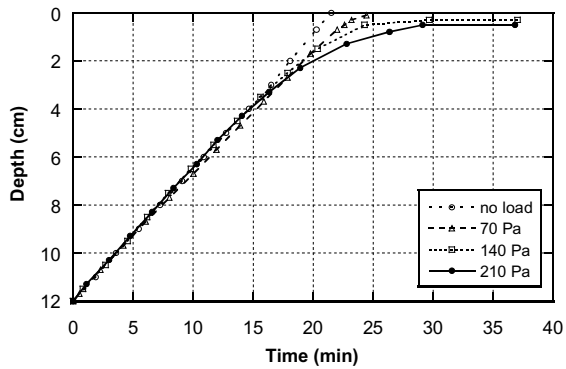

Fig. 7. The ascent of a crack upper tip under the influence of a surface load. A crack containing 15 ml liquid vertically ascended just under a surface load. The surface load per unit area was varied from 0 to 210 Pa. Without a surface load, a crack ascended at a nearly constant rate. With a surface load, a significant decrease in the ascent velocity was observed at the depth less than 5 cm. The velocity drop is more significant for a larger surface load.
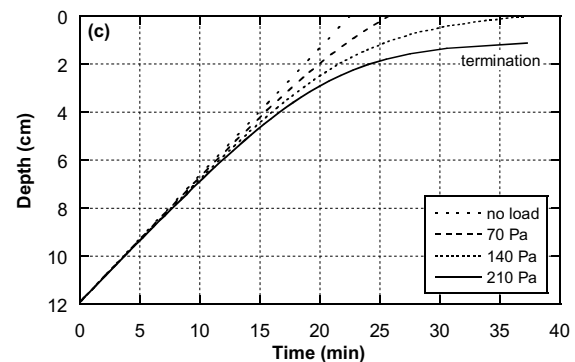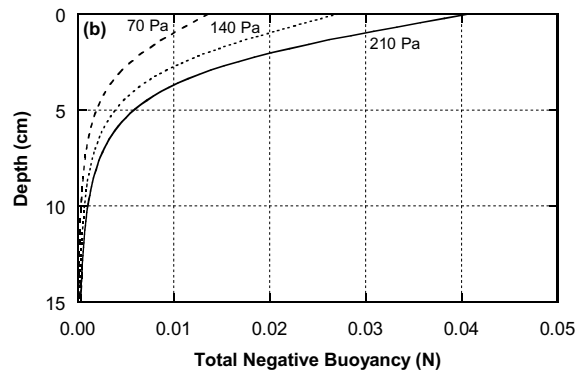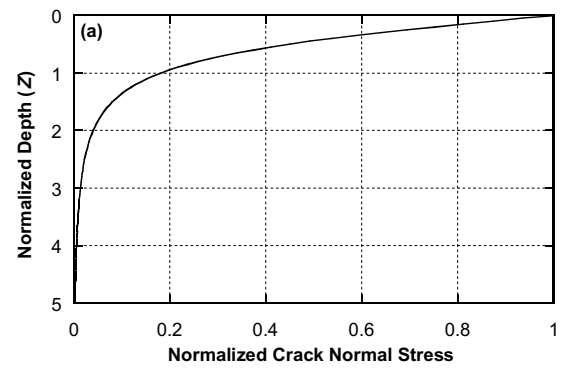

Fig. 8. (a) The depth profile of the crack normal stress. The normal stress is generated by a surface load and is analytically evaluated as shown in Appendix A. The depth is normalized by the half-width of a load, and the normal stress by the surface load per unit area. (b) The depth profile of the total negative buoyancy of a crack containing 15 ml liquid. The negative buoyancy was evaluated by the integration of the vertical gradient of the crack normal stress along the crack height. For simplicity, we assumed that the width and the thickness of a crack are constant along its height. The surface load per unit area is varied as 70, 140 and 210 Pa as in experiments. (c) The ascent of a crack upper tip under the influence of a surface load. The ascent velocity was calculated by using the total negative buoyancy shown in Fig. 8(b), assuming that the resistant force is proportional to the velocity and that the proportionality coefficient is independent of the buoyancy.

cracks through the stress around it. The interaction between open cracks was studied in material science first (e.g., Yokobori *et al.*, 1965). Later, the interaction between pressured cracks was studied and applied to geological phenomena such as dikes and spreading ridge segments (e.g., Delaney and Pollard, 1981). In a pressured crack, a crack-filling liquid has higher pressure than the surrounding but no buoyancy. Takada (1994a, b) studied the interaction between buoyancy-driven cracks both experimentally and theoretically, and applied the results to the interaction of ascending dikes. He demonstrated that the interaction of buoyancy-driven cracks can lead to the coalescence of ascending dikes, and proposed it as a mechanism of magma accumulation.

The style of the interaction between two buoyancy-driven cracks varies with the arrangement of two cracks: perpendicular, collinear and parallel (Takada, 1994b). Parallel cracks must be most common arrangement, because they tend to be perpendicular to the least compressive direction of the regional stress field before approaching other cracks. If the regional stress is sufficiently large in the intensity, it reduces the influence of stresses generated by the preceding crack and suppresses the crack interaction (Takada, 1994a).

The crack interaction can play an important role in magma transport, if the intensity of the regional stress is sufficiently low. When a following crack approaches the preceding one, it will change its propagation direction under the influence of stresses generated by the preceding one. The directional change reflects characteristics of the stress field around the preceding crack.

Characteristics of the stress field around a three-dimensional buoyancy-driven crack can be understood based
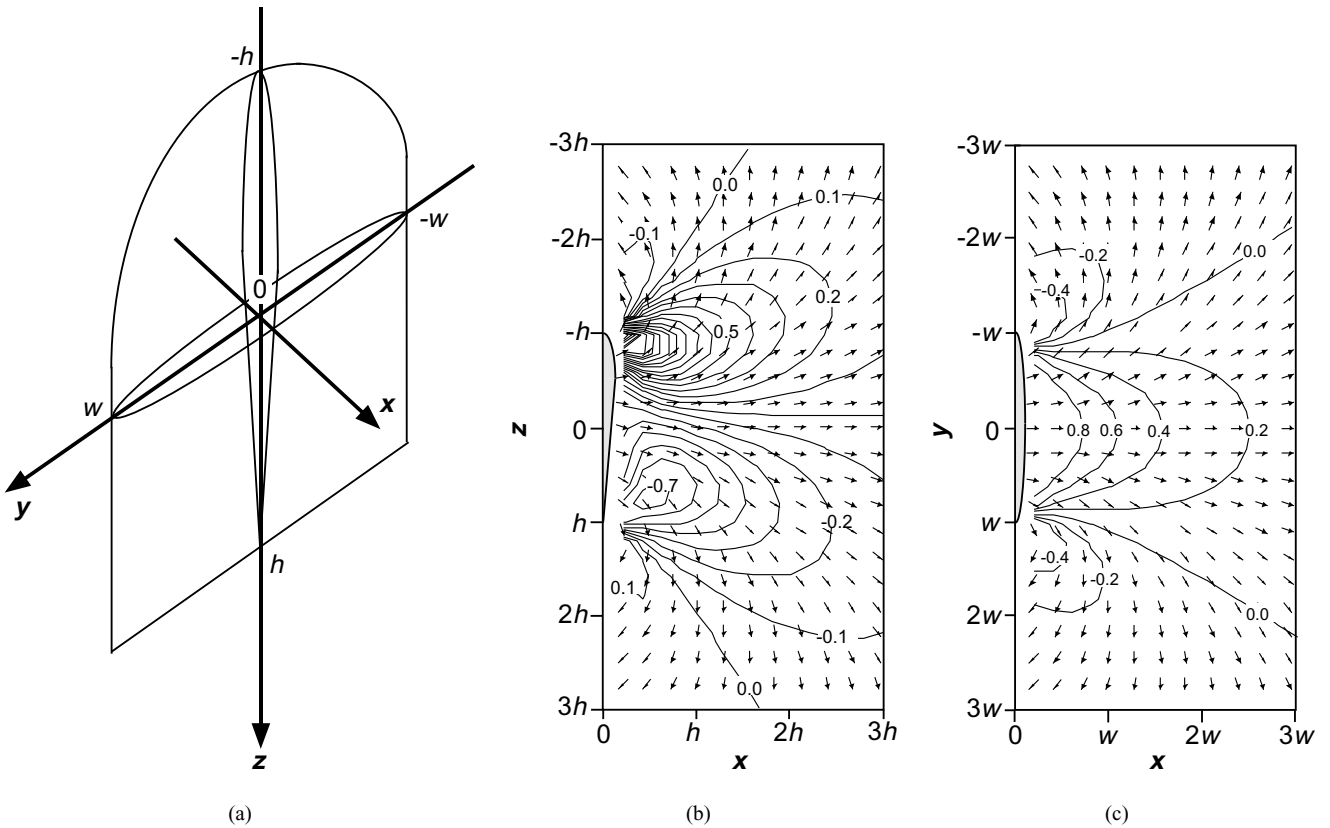
Fig. 9. (a) A schematic drawing of a three-dimensional buoyancy-driven vertical crack. The coordinate used in Figs. 9(b) and (c) is defined as shown. The half-height and half-width are denoted by h and w, respectively. (b) The direction of the maximum compressive stress and the contour of the shear stress σ'_{zx} around a two-dimensional buoyancy-driven crack. The stress distribution was analytically evaluated by following the stress function method (Westergaard, 1939). The shear stress is normalized by the average liquid excess pressure. (c) The direction of the maximum compressive stress and the contour of the stress σ'_{xx} around a two-dimensional pressured crack. The liquid pressure is assumed to be uniform. The stress distribution was analytically evaluated by following the stress function method (Westergaard, 1939). The stress value is normalized by the liquid excess pressure.

on the stress field around two-dimensional cracks. Let us consider a three-dimensional buoyancy-driven vertical crack (see Fig. 9(a)). The stress distribution in a vertical plane (z-x plane) is similar to that around a two-dimensional buoyancy-driven crack (Fig. 9(b)). The direction of the maximum compressive stress and the contour of the shear stress σ_{zx}, which is normalized by the average liquid excess pressure, are shown. The shear stress will change the orientation of a following crack from vertical to parallel to the maximum compressive stress. This results in the bending toward the preceding crack. The stress distribution in a horizontal plane (x-y plane) is similar to that around a two-dimensional pressured crack (Fig. 9(c)). The direction of the maximum compressive stress and the contour of the stress σ_{xx}, which is normalized by the liquid excess pressure at the depth, are shown. The stress σ_{xx} changes steeply in the direction parallel to the crack (y-direction). The change in the stress σ_{xx} is gradual in the direction perpendicular to the crack (x-direction). If there is an offset between two cracks (see Fig. 3), the horizontal gradient of the stress σ_{xx} will cause the horizontal pressure gradient in the following crack. This leads to migration in the y-direction, which we hereafter call horizontal migration. Reflecting the stress distribution around the first one (Fig. 9(c)), the liquid pressure in the second crack is higher at the side near the center of the first crack. The horizontal migration thus occurs in the outward direction from

the first one.

Previous studies (e.g., Takada, 1994a, b) showed that bending toward the first crack can lead to coalescence of cracks. If the horizontal distance between cracks is not so large, the second crack propagates to cut the wall of the first crack and injects its liquid into the first one. The second crack then closes and the first one grows. However, those studies were limited to the two-dimensional interaction (with zero offset), and the condition for crack coalescence has not been understood quantitatively.

The purpose of Experiment 2 is to understand the condition for coalescence quantitatively in the three-dimensional space. Experiment 1 gives us a clue. It suggests that at least the ratio of the shear stress on the second crack to the average excess pressure must be larger than 0.2 for the second crack to be significantly deflected. Moreover, the stress distribution in a horizontal plane (Fig. 9(c)) suggests that the crack coalescence is more sensitive to the offset than the horizontal distance. The stress change is more gradual in the direction perpendicular to the crack than in the direction parallel to it. Experiment 2 was designed to test these considerations.

4.2 Method

Gelatin was prepared in a rectangular container (445 mm in width, 265 mm in depth and 325 mm in heights). Two liquid-filled cracks were formed sequentially without loading. The first crack was formed by injection of 7.5 ml sili-
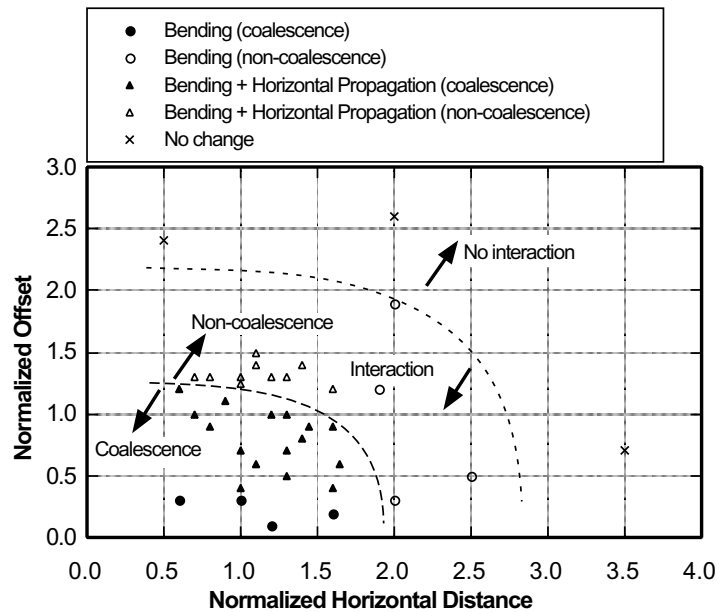
Fig. 10. Summary of the directional change of the second crack (Experiment 2). The configuration of two parallel cracks is shown in a diagram of the horizontal distance and the offset. The horizontal distance and the offset are both normalized by the half-width of the preceding crack. For larger horizontal distance and offset, no directional change of the second crack was observed. Namely, no interaction between two cracks was observed. For smaller horizontal distance and offset, a significant deflection of the second crack lead to the crack coalescence.

con oil. The height and the width were 60 mm and 50 mm, respectively. The ascent velocity was 2 mm/min. at the stationary state. After the first crack ascended about 6 cm, the second crack was formed parallel to the first one by injection of 10 ml silicon oil. Its position and orientation were deliberately controlled by the syringe needle. The height and the width were 65 mm and 55 mm, respectively. The second crack has the average liquid excess pressure of 8% higher than the first one. At the stationary state, its ascent velocity was 2.8 mm/min. With above conditions the second crack could pass the first one during its ascent in gelatin.

The horizontal distance and the offset between two cracks (see Fig. 3) were measured when the second crack was completely injected. At that time, both cracks were vertical. We observed two cracks for various horizontal distance and offset. The horizontal distance was varied from $0.5w$ to $3.5w$ ($w = 25$ mm: the half width of the preceding crack), and the offset from $0.1w$ to $2.6w$.

4.3 Results and discussion

The behaviour of the second crack is summarized in Fig. 10. Directional changes were observed for the horizontal distance less than $2.5w$ and the offset less than $2.0w$. The horizontal distance and offset are defined in Fig. 3. No significant directional change was observed outside this region. The crack coalescence was observed for the horizontal distance less than $2.0w$ and the offset less than $1.2w$. In the region between curves of coalescence and no interaction, the second crack deflected significantly but could not reach the first one during passing.

Typical examples of the directional change are shown in Fig. 11. The style of the directional change varies with the offset. For small offset ($<0.2w$), the second crack bends its upper tip uniformly toward the first one (Fig. 11(a): horizontal distance $= 1.2w$, offset $= 0.1w$), leading to coalescence.

No significant horizontal migration was observed. A small offset can generate no significant horizontal pressure gradient to cause the horizontal motion.

For larger offset ($>0.2w$), significant horizontal migration is observed in addition to bending (Fig. 11(b): horizontal distance $= 1.6w$, offset $= 0.9w$). The amount of horizontal migration is maximized at the offset of around w. The maximum value is $0.2w$ in our experiments. When the horizontal distance is larger than 1.8, the horizontal migration was not observed. It should be due to a small horizontal gradient of the crack normal stress at a large horizontal distance (Fig. 9(c)).

For the offset larger than $1.0w$, the amount of upper tip bending varies significantly along the width of the second crack. It increases with approaching the center of the first crack. This might be due to the horizontal gradient of the shear stress on the second crack. This differential rotation of the upper tip results in a rotation of the crack plane around the vertical direction. An example of the differential rotation is shown in Fig. 11(c) (horizontal distance $= 1.0w$, offset $= 1.3w$).

The observed extent of crack interaction can be understood based on the stress distribution around the first crack. Experiment 1 has shown that a significant deflection occurs when the ratio of the shear stress to the average excess pressure is larger than 0.2. The distribution of the shear stress around the first crack is shown in Fig. 9(b), in which the stress is normalized by the average excess pressure of the first crack. In our experiments, the height and width of the first crack are 60 and 50 mm. The average excess pressure of the second crack is higher than that of the first one by 8%. First, let us consider the case with zero offset. The ratio of the shear stress to the average excess pressure of the second crack can be higher than 0.2, if the horizontal distance is less
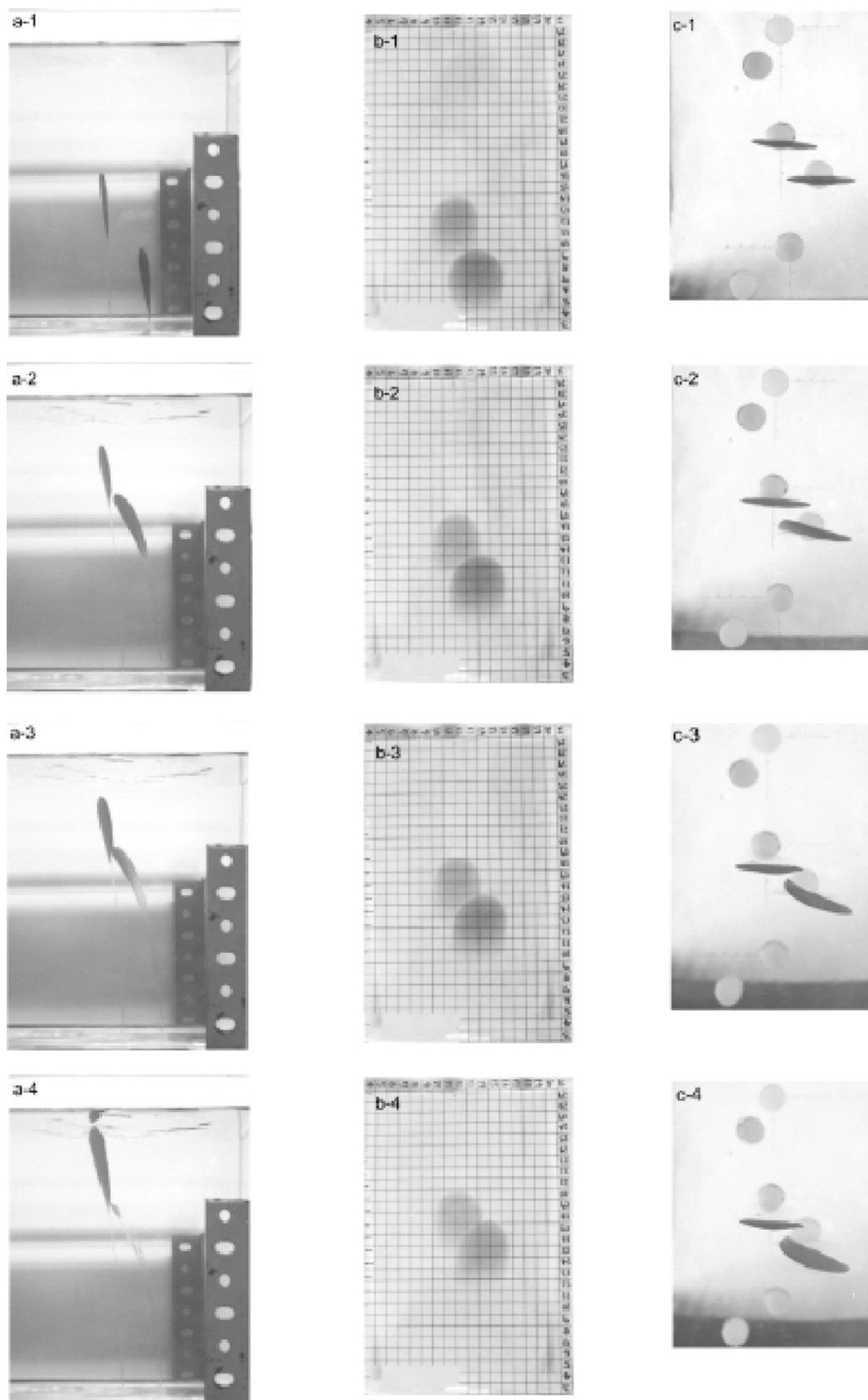
Fig. 11. (a) Photographs showing the bending of the second crack (in a vertical plane perpendicular to the crack plane). The horizontal distance and the offset are 1.2 and 0.1 in the normalized scale. The upper tip of the second crack uniformly bended toward the first one, and the two cracks coalesced to one large crack. (b) Photographs showing the horizontal propagation of the second crack (in a vertical plane parallel to the crack plane). The horizontal distance and the offset are 1.6 and 0.9 in the normalized scale. In addition to the horizontal propagation, the second crack bended its upper tip to the preceding one, resulting in the crack coalescence. (c) Photographs showing the differential rotation of the upper tip of the second crack (right). They are taken from the top. The horizontal distance and the offset are 1.0 and 1.3 in the normalized scale. The amount of bending of the upper tip is larger close to the center of the first crack. This differential rotation of the upper tip results in a rotation of the crack plane around the vertical direction. Although the second crack changed its orientation, it passed the first one without the coalescence.

than $2.7w$ (w: the width of the first crack). When the offset is sufficiently small, the second crack deflects from the vertical direction under the influence of the shear stress generated by the first crack. As the offset increases, the shear stress on the second crack steeply decreases. It will diminish the horizontal extent of crack interaction.

The observed extent of crack interaction must depend on the volume ratio of cracks. Since the extent of crack interaction depends on the ratio of the shear stress to the average excess pressure of the second crack, it will be smaller as the second crack has higher excess pressure.

The extent for coalescence must also depend on the volume ratio of two cracks. The obtained condition (the horizontal distance $< 2.0w$, the offset $< 1.2w$) can only be applied to the case where the volume ratio of the second crack to the first one is 1.33. As the volume ratio becomes larger, the ratio of the shear stress to the average excess pressure of the second crack becomes smaller and the duration time for passing shorter. The extent of crack coalescence will shrink.

The extent for coalescence must vary with the fluid in the second crack. If the second crack contains a less dense fluid, the average excess pressure of the second crack becomes higher and the duration time for passing shorter. The extent of coalescence will shrink.

The extent of crack coalescence has directivity, while it depends on the volume ratio and the content of cracks: the extent is more sensitive to the offset than the horizontal distance. The implication will be discussed in the Subsection 5.3.

5. Implication for Magma Ascent and Emplacement

5.1 Volcanism in compressional stress fields

In view of crack propagation, volcanism in a compressional stress field, in which the maximum tensile stress is nearly in the vertical direction, has been puzzling. Since a vertical magma-filled crack is not perpendicular to the maximum tensile stress, it is directionally unstable (e.g., Cotterell and Rice, 1980). It will deflect its orientation progressively, and finally become horizontal. The magma will be emplaced at this level in spite of its buoyancy. Thus, it seems impossible for magmas to ascend to the Earth's surface through cracks. However, the degree of crack deflection is expected to depend on the relationship between the external stress and the magma excess pressure. A crack with higher magma excess pressure will ascend to a higher level in the lithosphere. Our results of Experiment 1 support this idea. When the ratio of the shear stress on a crack plane to the average magma excess pressure is sufficiently small, no significant deflection is expected.

A magma-filled crack generates at the deep in the lithosphere; probably the uppermost mantle (e.g., Rubin, 1998). Since the stress state there is nearly hydrostatic, a vertical crack will gradually deflect its orientation. The compressional stress increases with the ascent of magma, and the crack accelerates its deflection to be horizontal. The magma ceases its ascent and is emplaced there. The level of magma emplacement is thus controlled by the relationship between the external shear stress and the average magma excess pressure.

If magma cools and becomes too viscous to flow, it ceases its ascent during the deflection of its crack plane. Significant S-wave reflection observed beneath active volcanoes (e.g., Matsumoto and Hasegawa, 1996) could be caused by such magma bodies. Observed reflective bodies often have dip angles around 30°. Host rocks will be heated by repeated intrusion of magmas and then the magnitude of the tectonic stress will be locally reduced. Following magmas can ascend higher to cause surface activities. Tectonic forces will be supported by the surrounding region. The seismicity in volcanic regions (e.g., Hasegawa *et al.*, 1991) may reflect such tectonic and thermal processes. Combined study of geophysical observations and numerical modeling will lead to a good understanding of volcanism in relation to its tectonic environment.

5.2 Influences of topographic load

The topographic load generates a gravitational stress, which can be a principal component of the external stress at shallow levels ($<$a few km). The gravitational stress affects the ascent and emplacement of magmas in two ways. First, it affects the orientation of magma-filled cracks to govern the array of vents and the site of eruption. Secondly, the gradient of the crack normal stress changes the driving force of ascent to control the depth of emplacement.

The influence on the orientation of dikes has been often pointed out. Fiske and Jackson (1972) performed gelatin experiments to study the crack propagation in a volcanic edifice, and showed that the gravitational stress played an important role in controlling the orientation and growth of Hawaiian volcanic rifts. McGuire and Pullen (1989) investigated the distribution and orientation of fissures at Mt. Etna, and showed that the competition between the gravitational stress and the regional tectonic stress determined the location and orientation of eruptive fissures and feeder-dikes. Muller *et al.* (2001) performed both laboratory and numerical experiments to investigate the influence of a volcanic load on the crack propagation in the basement. The surface load can attract an ascending dike. They defined the critical distance as the maximum distance from which the load attracts a dike, and obtained an empirical relation between the critical distance and the ratio of the load per unit area to the magma driving pressure. They applied their results to explain the spacing and sizes of volcanoes in the Cascade Range. Their results are consistent with our Experiment 1. Since the volume of crack-filling liquid was fixed, the average liquid excess pressure was constant in their experiments. As the distance from the surface load increases, the intensity of the external stress and the degree of crack deflection decrease. The ratio of the maximum shear stress on a crack plane to the average excess pressure must be less than 0.2 for a crack without deflection.

The gradient of crack normal stress has been pointed out to affect magma ascent. Rubin (1995) made a comprehensive review on the role of stress gradient. Our experiments (Experiment 1) have shown that the topographic load reduces the driving force of magma ascent through the stress gradient. It can change the emplacement depth of magmas. Pinel and Jaupart (2000) studied the influence of the gravitational stress on magma ascent and showed that a volcanic edifice can work as a magma filter that prevents the eruption
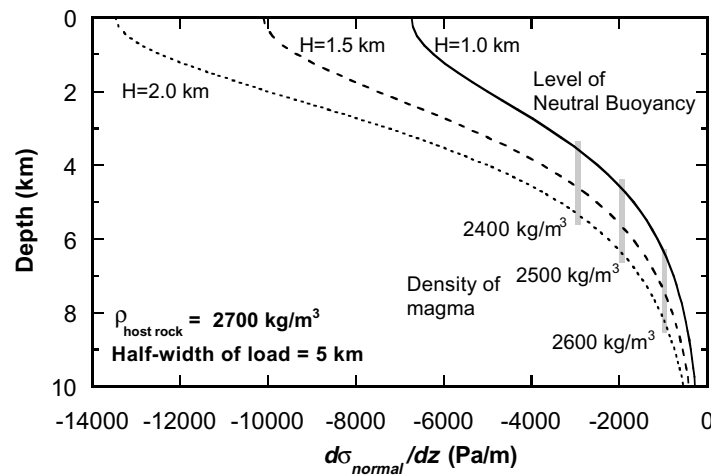
Fig. 12. The vertical gradient of the crack normal stress induced by a mountain load. The load is assumed to be in a two-dimensional simple geometry (10 km width and a uniform height). The height is varied as 1.0, 1.5 and 2.0 km. The crack is assumed to ascend vertically beneath the center of the load. The density of host rocks is assumed to be uniformly 2700 kg/m³. The intercept of a stress gradient and a thick vertical line indicates the level of neutral buoyancy (the emplacement depth).

of dense magmas. Their discussion was, however, based on the static criterion for a crack to extend (e.g., Watanabe *et al.*, 1999). The pressure distribution in a crack was assumed to be hydrostatic. As Lister and Kerr (1991) showed, once a crack begins to extend, the pressure distribution is dynamically determined. Here, we evaluate the influence of a mountain load on the emplacement depth of magma by applying the effect of stress gradient to a dynamically ascending crack.

The vertical gradient of the crack normal stress is calculated for a mountain load with two-dimensional simple geometry (10 km width and a uniform height). The crack is assumed to ascend vertically beneath the center of the load. The formulation used for this calculation is described in Appendix A. The density of host rocks is assumed to be uniformly 2700 kg/m³. The depth profile of the stress gradient is shown in Fig. 12. The negative value implies more compressive stress at shallower levels. Thus, the stress gradient works as negative buoyancy. The magnitude of the stress gradient rapidly increases with ascent at shallow levels (<5 km), and it increases with the mountain height.

The emplacement depth is given as LNB. We consider a crack to which magma is continuously injected from the bottom, because previous studies (e.g., Nakashima, 1993) have shown that an isolated crack can contain only a small volume of magma and cannot play a major role in the magma transport due to rapid freezing. Lister and Kerr (1991) have shown that a continuously injected crack changes its propagation direction from vertical to horizontal at LNB. When the magma supply terminates, magma is emplaced around there.

The buoyancy comes from the density difference between magma and host rocks and the vertical gradient of crack normal stress:

$$f = \Delta\rho g + \frac{d\sigma_{normal}}{dz}.$$

If the negative buoyancy due to stress gradient equals the buoyancy due to density difference in magnitude, a magma-filled crack will cease to ascend. LNB is shown in Fig. 12

for various density of magma. When the magma density is 2400 kg/m³ (the density difference of 300 kg/m³), the emplacement depth will be 3∼5 km. The emplacement depth becomes deeper for higher mountain loads. If a volcanic edifice grows to the height of 2 km, magmas cannot reach to the surface without a large reduction of the density (∼1000 kg/m³). If the magma density is 2600 kg/m³, the vesiculation around 40 vol.% is needed to decrease the density by 1000 kg/m³. Though other stress sources as regional tectonic forces may reduce the effect of a mountain load, we must stress that the topographic load can affetcs the evolution of eruption style during the lifetime of a volcano.

5.3 Magma mixing by crack coalescence

Petrological studies have shown that mechanical mixing of magmas with different compositions often occurs beneath volcanoes (e.g., Nakamura, 1995). The crack coalescence is one of viable mechanisms for magma mixing. If the tectonic stress is weak enough, magma-filled cracks can coalesce repeatedly in the course of magma ascent: from deep in the lithosphere to the Earth's surface.

Our experiment has shown that crack coalescence has directivity. It can affect the spatial variation in chemistry of erupted and intruded magma. Magma mixing through crack coalescence can take place more easily in the direction perpendicular to the preceding crack than in the direction parallel to it. Most of cracks should be perpendicular to the maximum tensile direction, even if the stress magnitude is very low. Thus, the spatial variation of magma chemistry is more diminished in the direction of the maximum tensile stress than in the direction perpendicular to it. The directivity should be taken into account in interpretation of the spatial variation of magma chemistry.

6. Conclusions

If a liquid-filled crack is not perpendicular to the maximum tensile stress, it propagates with progressively changing its orientation. It tends to be perpendicular to the maximum tensile stress. The degree of deflection reflects the competition between the external stress and the liquid excess

pressure. When the ratio of the shear stress on a crack plane to the average excess pressure is less than 0.2, no significant deflection takes place. The volcanic activity in a compressional stress field might be understood in the context of this competition.

A mountain load generates a stress gradient along a crack, which can significantly change the driving force of propagation. The stress gradient can control the emplacement depth of magmas. It might lead to the evolution of eruption style during the lifetime of a volcano.

An ascending crack can be a source of external stress to a following crack. It changes the propagation direction of a following crack, and can lead to the coalescence of two cracks. The deflection of a following crack takes place, when the ratio of the shear stress generated by the preceding crack to the average excess pressure of the following crack is larger than 0.2. The coalescence takes place in a smaller area. It has directivity: the region of coalescence extends more in the direction perpendicular to the preceding crack than in the direction parallel to it. It reflects the stress field around the preceding crack. This directivity might cause a characteristic spatial variation of magma chemistry through magma mixing.

Appendix A. Non-Hydrostatic Stress Generated by Surface Load

Let us suppose two-dimensional situation shown in Fig. A1. A surface load is uniformly distributed at $-a < x < +a$ (a: the half width of the load). The stress generated by the load can be analytically evaluated as follows (e.g., Jaeger, 1969).

$$\sigma'_{xx} = \frac{P}{\pi}\left[(\theta_1 - \theta_2) - \frac{(x+a)z}{(x+a)^2 + z^2} + \frac{(x-a)z}{(x-a)^2 + z^2}\right] \tag{A.1}$$

$$\sigma'_{zz} = \frac{P}{\pi}\left[(\theta_1 - \theta_2) + \frac{(x+a)z}{(x+a)^2 + z^2} - \frac{(x-a)z}{(x-a)^2 + z^2}\right] \tag{A.2}$$

$$\sigma'_{xx} = \frac{P}{\pi}\frac{z^2(r_2^2 - r_1^2)}{r_1^2 r_2^2} \tag{A.3}$$

where P is the load per unit area. From (A.1), the vertical gradient of σ'_{xx} is expressed as

$$\frac{d\sigma'_{xx}}{dz} = \frac{P}{\pi}\left[\frac{2a(x^2 - z^2 - a^2)}{[(x+a)^2 + z^2][(x-a)^2 + z^2]}\right.$$
$$- \frac{(x+a)[(x+a)^2 - z^2]}{[(x+a)^2 + z^2]}$$
$$\left. + \frac{(x-a)[(x-a)^2 - z^2]}{[(x-a)^2 + z^2]}\right] \tag{A.4}$$

The contour of the vertical gradient is shown in Fig. A2. The magnitude of the vertical gradient is normalized by the ratio of the load per unit area to the half-width of the load. At
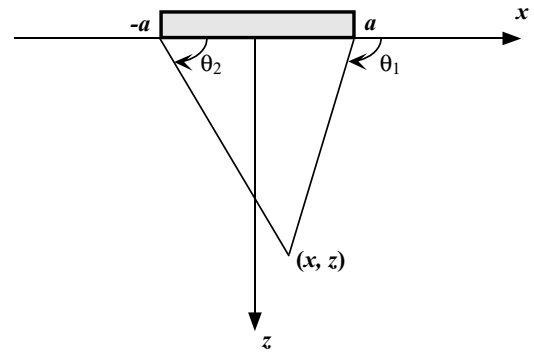

Fig. A1. The definition of the coordinate and angles (θ_1 and θ_2) used in the calculation of the stress generated by a surface load ($-a < x < a$).

$x = 0$, we obtain

$$\frac{d\sigma'_{xx}}{dz} = -\frac{4P}{\pi a}\frac{1}{[1 + (z/a)^2]^2}. \tag{A.5}$$

Appendix B. The Liquid Excess Pressure in a Vertically Ascending Crack

The liquid pressure p_l is approximately hydrostatic in our experiments, since the flow in a crack is laminar and the viscous pressure drop is negligible. The liquid pressure in a vertically ascending crack is thus given as

$$p_l(z) = p_l(z_0) + \rho_l g(z - z_0) \tag{B.1}$$

where z_0 and ρ_l are the depth of the crack center and the density of the liquid. It will be shown in the following that the flow is laminar and the viscous pressure drop is negligible.

The laminar flow is justified from the Reynolds number,

$$Re = \frac{\rho_l t v}{\eta} \tag{B.2}$$

where η, t and v are the viscosity of the liquid, the average half thickness and the ascending velocity of a crack. Dimensions of a crack are defined as Fig. 3. The flow is laminar if the Reynolds number is smaller than ~ 1000 (e.g., Spence and Turcotte, 1990). In our experiments, the average half thickness is around 3 mm, and cracks ascend at nearly constant rate (~ 10 mm/min.). The Reynolds number is calculated to be around 0.5.

The viscous pressure drop per unit length is given by

$$\Delta P_v = \frac{\eta v}{t^2} \tag{B.3}$$

(e.g., Lister and Kerr, 1991). This is calculated to be around 0.07 Pa/m, which is much smaller than the hydrostatic pressure gradient $\rho_l g$ (8000 Pa/m).

The crack normal stress is composed of hydrostatic and deviatoric components as

$$\sigma(z) = \sigma(z_0) + \int_{z_0}^{z}\left(\rho_g g + \frac{d\sigma'_{xx}}{dz}\right)dz \tag{B.4}$$

where ρ_g and σ'_{xx} are the density of gelatin and the deviatoric stress. If the second term in the integral is negligible
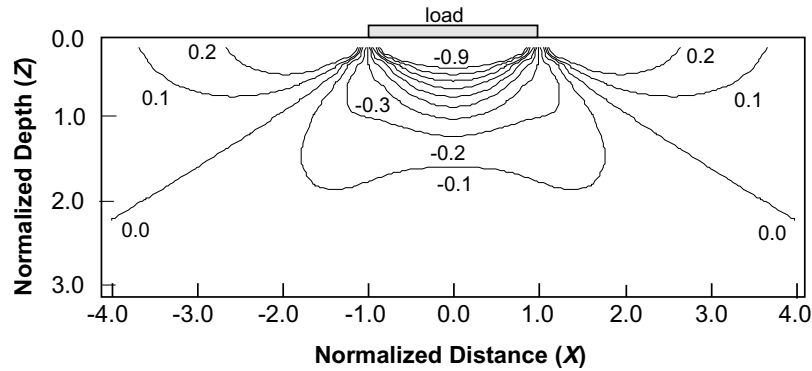
Fig. A2. The contour of the vertical gradient of σ'_{xx}. The magnitude of the gradient is normalized by the ratio of the load per unit area to the half-width of the load.

compared with the first term, the liquid excess pressure is approximately expressed as

$$p_{ex}(z) = [p_l(z_0) - \sigma(z_0)] - (\rho_g - \rho_l)g(z - z_0). \quad \text{(B.5)}$$

The average excess pressure is thus given by

$$\bar{p_{ex}} = p_l(z_0) - \sigma(z_0). \quad \text{(B.6)}$$

Secor and Pollard (1975) showed that the average excess pressure on the verge of propagation is related to the crack height L as

$$\bar{p_{ex}} = \frac{(\rho_g - \rho_l)gL}{4}. \quad \text{(B.7)}$$

From (B.4), the approximation (B.5) is valid when

$$\left|\frac{d\sigma'_{xx}}{dz}\right| \ll \rho_g g. \quad \text{(B.8)}$$

The magnitude of the vertical gradient is shown in Fig. A2, in which the normalizing factor is of the order of 2×10^3 Pa/m. The magnitude of $\rho_g g$ is around 10^4 Pa/m. If the normalized depth is larger than 1, the L.H.S. is less than the R.H.S. by two orders of magnitude.

References

Cotterell, B. and J. R. Rice, Slightly curved or kinked cracks, *Int. J. Fract.*, **16**, 155–169, 1980.

Delaney, P. T. and D. D. Pollard, Deformation of host rocks and flow of magma during growth of minette dikes and breccia-bearing intrusion near Ship rock, New Mexico, *U.S. Geol. Surv. Prof. Pap.*, **1202**, 1–61, 1981.

Delaney, P. T., D. D. Pollard, J. I. Ziony, and E. H. McKee, Field relations between dikes and joints: emplacement processes and paleostress analysis, *J. Geophys. Res.*, 4920–4938, 1986.

Emerman, S. H., D. L. Turcotte, and D. A. Spence, Transport of magma and hydrothermal solutions by laminar and turbulent fluid fracture, *Phys. Earth Planet. Inter.*, **41**, 249–259, 1986.

Fiske, R. S. and E. D. Jackson, Orientation and growth of Hawaiian volcanic rifts: the effect of regional structure and gravitational stresses, *Proc. R. Soc. Lond. A*, **329**, 299–326, 1972.

Hasegawa, A., D. Zhao, S. Hori, A. Yamamoto, and S. Horiuchi, Deep structure of the northeastern Japan arc and its relationship to seismic and volcanic activity, *Nature*, **352**, 683–689, 1991.

Heimpel, M. and P. Olson, Buoyancy-driven fracture and magma transport through the lithosphere: models and experiments, in *Magmatic Systems*, edited by M. P. Ryan, pp. 223–240, Academic Press, San Diego, 1994.

Hyndmann, D. W. and D. Alt, Radial dikes, laccoliths, and gelatin models, *J. Geol.*, **95**, 763–774, 1987.

Ida, Y., Effects of the crustal stress on the growth of dikes: Conditions of intrusion and extrusion of magma, *J. Geophys. Res.*, **104**, 17897–17909, 1999.

Jaeger, J. C., *Elasticity, Fracture, and Flow*, 3rd ed., 268 pp., Methuen, London, 1969.

Lawn, B., *Fracture of Brittle Solids*, 2nd ed., 378 pp., Cambridge University Press, Cambridge, 1993.

Lister, J. R., Buoyancy-driven fluid fracture: similarity solutions for the horizontal and vertical propagation of fluid-filled cracks, *J. Fluid Mech.*, **217**, 213–239, 1990.

Lister, J. R., Steady solutions for feeder dykes in a density-stratified lithosphere, *Earth Planet. Sci. Lett.*, **107**, 233–242, 1991.

Lister, J. R. and R. C. Kerr, Fluid-mechanical models of crack propagation and their application to magma transport indykes, *J. Geophys. Res.*, **96**, 10049–10077, 1991.

Maaløe, S., The generation and shape of feeder dykes from mantle sources, *Contrib. Mineral. Petrol.*, **96**, 47–55, 1987.

Matsumoto, S. and A. Hasegawa, Distinctive S wave reflector in the mid-crust beneath Nikko-Shirane volcano in the northeastern Japan arc, *J. Geophys. Res.*, **101**, 3067–3083, 1996.

McGuire, W. J. and A. D. Pullen, Location and orientation of eruptive fissures and feeder dykes at Mount Etna; influence of gravitational and regional stress regimes, *J. Volcanol. Geotherm. Res.*, **38**, 325–344, 1989.

Mériaux, C. and C. Jaupart, Dike Propagation through an elastic plate, *J. Geophys. Res.*, **103**, 18295–18314, 1998.

Muller, J. R., G. Ito, and S. J. Martel, Effects of volcano loading on dike propagation in an elastic half-space, *J. Geophys. Res.*, **106**, 11101–11113, 2001.

Nakamura, K., Volcanoes as possible indicators of tectonic stress orientation, *J. Volcanol. Geotherm. Res.*, **2**, 1–16, 1977.

Nakamura, M., Continuous mixing of crystal mush and replenished magma in the ongoing Unzen eruption, *Geology*, **23**, 807–810, 1995.

Nakashima, Y., Static stability and propagation of a fluid-filled edge crack in rock: implications for fluid transport in magmatism and metamorphism, *J. Phys. Earth*, **41**, 189–202, 1993.

Pinel, V. and C. Jaupart, The effect of edifice load on magma ascent beneath a volcano, *Phil. Trans. R. Soc. Lond. A*, **358**, 1515–1532, 2000.

Pollard, D. D. and A. M. Jackson, Mechanics and growth of some laccolithic intrusions in the Henry mountains, Utah, II, *Tectonophys.*, **18**, 311–354, 1973.

Pollard, D. D. and O. H. Muller, The effect of gradients in regional stress and magma pressure on the form of sheet intrusions in cross section, *J. Geophys. Res.*, **81**, 975–984, 1976.

Pollard, D. D. and G. Holzhausen, On the mechanical interaction between a fluid-filled fracture and the earth's surface, *Tectonophys.*, **53**, 27–57, 1979.

Richards, R. and R. Mark, Gelatin models for photoelastic analysis of gravity structures, *Exp. Mech.*, **6**, 30–38, 1966.

Rubin, A. M., Propagation of magma-filled cracks, *Annu. Rev. Earth Planet. Sci.*, **23**, 287–336, 1995.

Rubin, A. M., Dike ascent in partially molten rock, *J. Geophys. Res.*, **103**, 20901–20919, 1998.

Secor, D. T. and D. D. Pollard, On the stability of open hydraulic fractures in the Earth's crust, *Geophys. Res. Lett.*, **2**, 510–513, 1975.

Sparks, R. S., H. Pinkerton, and R. MacDonald, The transport of xenoliths

in magmas, *Earth Planet. Sci. Lett.*, **35**, 234–238, 1977.

Spence, D. A. and D. L. Turcotte, Magma-driven propagation of cracks, *J. Geophys. Res.*, **90**, 575–580, 1985.

Spence, D. A., P. W. Sharp, and D. L. Turcotte, Buoyancy-driven crack propagation: a mechanism for magma migration, *J. Fluid Mech.*, **174**, 135–153, 1987.

Takada, A., Magma transport and reservoir formation by a system of propagating cracks, *Bull. Volcanol.*, **52**, 118–126, 1989.

Takada, A., Experimental study on propagation of liquid-filled crack in gelatin: shape and velocity in hydrostatic stress condition, *J. Geophys. Res.*, **95**, 8471–8481, 1990.

Takada, A., Accumulation of magma in space and time by crack interaction, in *Magmatic Systems*, edited by M. P. Ryan, pp. 241–257, Academic Press, San Diego, 1994a.

Takada, A., Development of a subvolcanic structure by the interaction of liquid-filled cracks, *J. Volcanol. Geotherm. Res.*, **61**, 207–224, 1994b.

Watanabe, T., T. Koyaguchi, and T. Seno, Tectonic stress controls on ascent and emplacement of magmas, *J. Volcanol. Geotherm. Res.*, **91**, 65–78, 1999.

Weertman, J., Theory of water-filled crevasses in glaciers applied to vertcal magma transport beneath oceanic ridges, *J. Geophys. Res.*, **76**, 1171–1183, 1971.

Westergaard, H. M., Bearing pressures and cracks, *Trans AIME, J. Appl. Mech.*, **6**, 49–53, 1939.

Yokobori, T., M. Ohashi, and M. Ichikawa, The interaction of two collinear asymmetrical elastic cracks, *Rep. Res. Inst. Strength Fract. Mat., Tohoku Univ.*, **1**, 33–39, 1965.

T. Watanabe (e-mail: twatnabe@sci.toyama-u.ac.jp), T. Masuyama, K. Nagaoka, and T. Tahara